RESEARCH ARTICLE



Molecular level characterization of DOM along a freshwater-to-estuarine coastal gradient in the Florida Everglades

Dennys Leyva¹ · Rudolf Jaffé² · Jessica Courson³ · John S. Kominoski⁴ · Muhammad Usman Tariq⁵ · Fahad Saeed^{5,6} · Francisco Fernandez-Lima^{1,2,6}

Received: 5 April 2022 / Accepted: 20 August 2022 / Published online: 23 September 2022 © The Author(s), under exclusive licence to Springer Nature Switzerland AG 2022

Abstract

Understanding dissolved organic matter (DOM) export to the ocean is needed to assess the impact of climate change on the global carbon cycle. The molecular-level characterization of DOM compositional variability and complexity in aquatic ecosystems has been analytically challenging. Advanced analytical studies based on ultra-high resolution mass spectrometry (FT ICR MS) have proven highly successful to better understand the dynamics of DOM in coastal ecosystems. In this work, the molecular signature of DOM along a freshwater-to-estuarine gradient in the Harney River, Florida Everglades was analyzed for the first time using a novel approach based on tandem high resolution ion mobility and ultra-high resolution mass spectrometry (ESI-TIMS-FT ICR MS). This method enhances traditional DOM molecular characterization by including the molecular isomeric complexity. An average of six and up to 12 isomers were observed per chemical formula and characteristic isomers to each section of the freshwater-to-estuarine gradient were successfully identified. We measured a decrease in the chemical complexity and diversity (both in the number of molecular formulas and number of isomers per chemical formula) with increasing salinity; this trend is representative of the biogeochemical transformations of DOM during transport and along source variations, showing both clear degradation products and formation of new components along the salinity transect. The inclusion of the isomeric content at the molecular formula allowed to differentiate isomeric species that are present along the transect (mainly lignin-type components) and responsible for the DOM refractory nature. DOM isomeric fingerprints characteristic of the molecular variability along the Everglades freshwater-to-estuarine gradient are also described.

 $\textbf{Keywords} \ \ TIMS-FT-ICR \ MS \cdot DOM \cdot Isomers \cdot Harney \ River \cdot ESI-TIMS-FT-ICR \ MS \cdot Molecular-level \ characterization \cdot Isomeric \ complexity \cdot Coastal \ ecosystem$

- Francisco Fernandez-Lima fernandf@fiu.edu
- Department of Chemistry and Biochemistry, Florida International University, Miami, FL 33199, USA
- Institute of Environment, Department of Chemistry and Biochemistry, Florida International University, Miami, FL 33199, USA
- Department of Chemistry, University of Louisiana at Lafayette, Lafayette, LA 70504, USA
- Institute of Environment, Department of Biological Sciences, Florida International University, Miami, FL 33199, USA
- School of Computing and Information Science, Florida International University, Miami, FL 33199, USA
- Biomolecular Sciences Institute, Florida International University, Miami, FL 33199, USA

Introduction

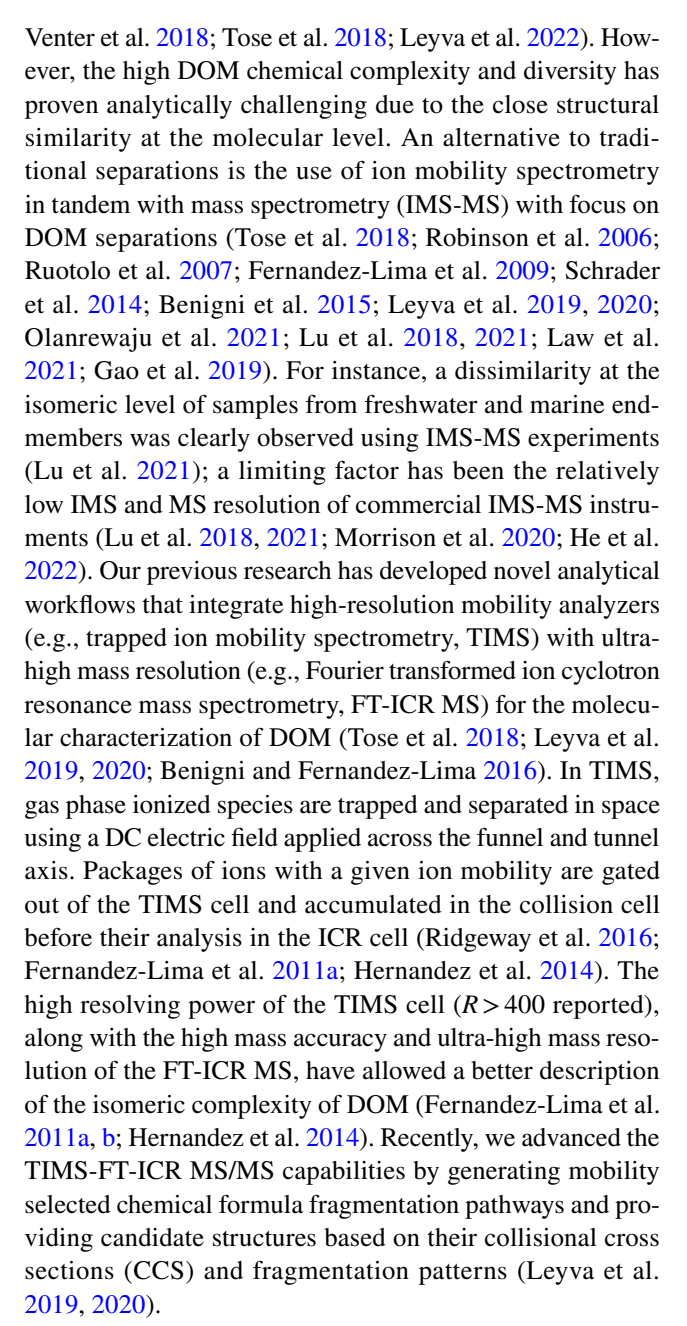
Dissolved organic matter (DOM) is a complex mixture of chemical compounds and constitutes a large quantity of organic carbon in aquatic ecosystems (Asmala et al. 2021; Buffam et al. 2011). The characterization of DOM has been widely used as a proxy to understand the biogeochemical dynamics of aquatic environments including complex phenomena such as the impact of land-use and climate change (Osterholz et al. 2016a; Wang et al. 2021; Berg et al. 2022; Zhang et al. 2022; Maie et al. 2014). In coastal wetlands, DOM has been the target of a multitude of studies due to the significant amount of organic carbon exported to the ocean (Zhang et al. 2022; Gonçalves-Araujo et al. 2015; Seidel et al. 2015; Hosen et al. 2018; Chow et al. 2013).



A wide variety of analytical techniques have been applied to obtain comprehensive information on the spatial and temporal variability of DOM in aquatic systems. Traditional measurements of dissolved organic carbon concentrations and other water quality parameters along with optical properties (UV-VIS and fluorescence) have been the most explored methods for bulk characterization of DOM (Wang et al. 2021; Fellman et al. 2010; Yamashita et al. 2013; Hansen et al. 2016; Gonçalves-Araujo et al. 2016; Clark et al. 2022; Zhang et al. 2018). More advanced analytical studies based on nuclear magnetic resonance (NMR) and ultra-high resolution mass spectrometry (FT-ICR MS) have proved to be critical to understanding chemical transformations of DOM and linking sources with compositional signatures (Kellerman et al. 2015; Roebuck et al. 2018; Seidel et al. 2014; Osterholz et al. 2015; Koch et al. 2005; Hertkorn et al. 2013).

The Florida Everglades is a complex mosaic of wetland ecosystems connected hydrologically through both natural and human-altered processes that are changing biogeochemical patterns across the landscape (Kominoski et al. 2020; Regier et al. 2020). Although several studies have approached the influence of environmental factors on the variability of DOM in the Everglades (Maie et al. 2014; Regier et al. 2020; Cawley et al. 2014; Yamashita et al. 2010; Chen et al. 2013; Regier and Jaffé 2016; Ya et al. 2015), few of them explored detailed molecular level analysis (Hertkorn et al. 2016; Wagner et al. 2015). For example, Hertkorn et al. (2016) conducted a comparison of DOM samples from various wetlands, including the Everglades, integrating optical properties including EEM-PARAFAC, as well as NMR and ultrahigh-resolution mass spectrometry demonstrating for the first time the extensive molecular diversity and compositional complexity of DOM in wetlands. Despite similar compositional patterns found across the samples, distinctive signatures could be explained by combinations of environmental drivers such as source variations, wildfires, and anthropogenic influences. Regarding the latter (mainly observed for CHOS species), anthropogenic sources associated with agriculture were primarily attributed to the singular DOM sulfur classes found. Combining optical properties, including PARAFAC fluorescence, and FT-ICR MS, Wagner et al. (2015) studied DOM from Shark River Slough and Taylor Slough in the Everglades. Several thousands of chemical compounds mainly distributed in the CHO, CHON, and CHOS heteroatom classes were detected across the samples and were closely correlated with the UV and fluorescent properties of the DOM, allowing for a good estimate of the origin and variability of DOM in this coastal ecosystem.

Recent efforts have increased the analytical power of ultra-high resolution mass spectrometry with the coupling of complementary separation techniques (Hawkes et al. 2016; Petras et al. 2017; Patriarca et al. 2018; Spranger et al. 2019;



Previous works have demonstrated the applicability of advanced analytical methods to advance our understanding of Everglades DOM biogeochemistry and have shown the necessity to further expand such studies and explore novel approaches to better understand how environmental drivers affect the DOM dynamics at the molecular level in vulnerable coastal ecosystems (Hertkorn et al. 2016; Wagner et al. 2015). Here, we conduct the first-ever characterization of the isomeric complexity of DOM along a freshwater-toestuarine gradient in the Harney River, Florida Everglades, using a novel approach based on tandem high resolution ion mobility and ultra-high resolution mass spectrometry (ESI-TIMS-FT ICR MS). Unique and common DOM molecular signatures have been successfully identified across the



transect as a proxy to understand biogeochemical processes, the role of input sources in DOM spatial variability, and DOM involvement in near coastal processes.

Experimental

Sample collection and treatment

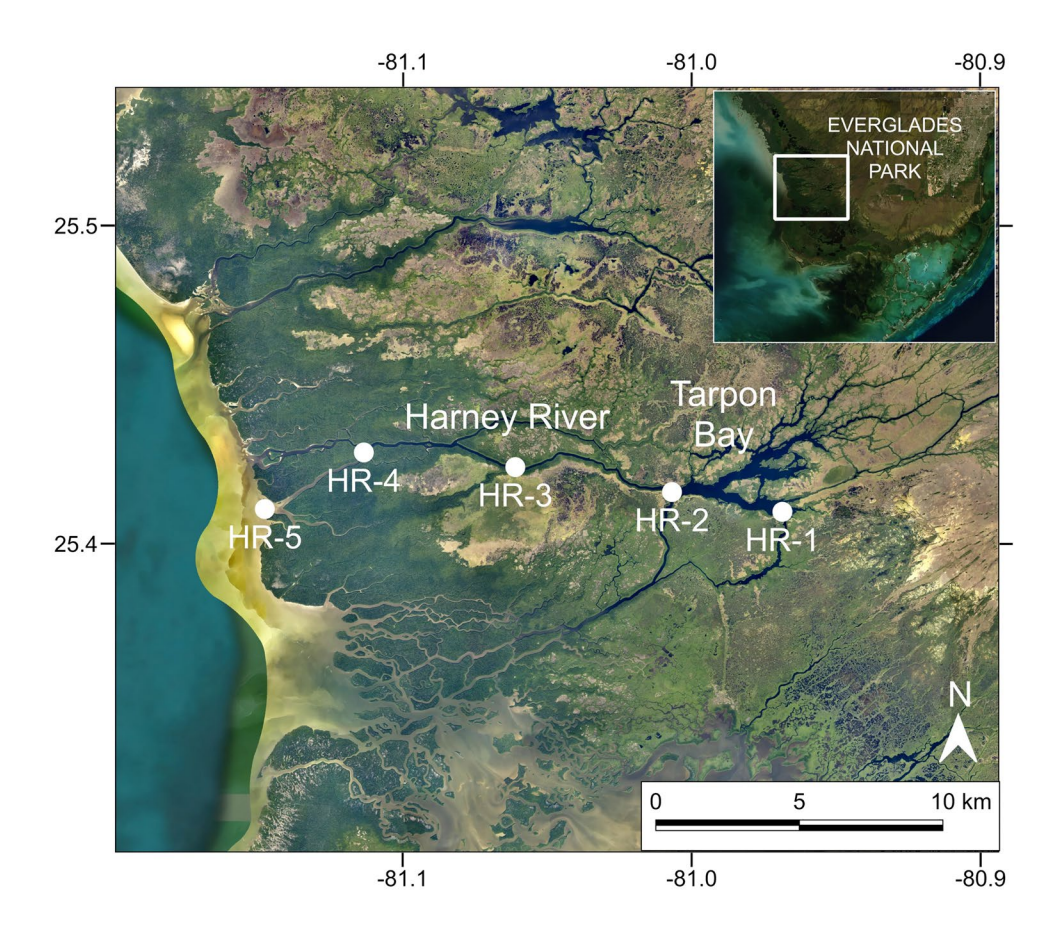
Water samples were collected along a salinity transect of the Harney River, Everglades National Park (Fig. 1), at the end of the subtropical dry season (April-May 2021). The Harney River exports fresh water from the upstream Everglades marshes, through a mangrove estuary, and out into the Gulf of Mexico. Salinity was measured on-site using a YSI sensor (YSI, Yellow Springs, OH, USA). Surface water was collected 50 cm below the surface and stored in HCl pre-washed 2 L amber plastic bottles (Nalgene®, Whaltham, MA, USA). Samples were kept on ice during transportation to the lab and filtered (0.22 µm, Whatman, Maidstone, UK) within 2 days after collection. Filtered samples were stored at 4 °C before treated by a solid-phase-extraction (SPE) procedure following the protocol developed by Dittmar et al. (2008). Briefly, one liter of sample previously acidified to pH 2 with Hydrochloric Acid was loaded onto a 1g-Bond Elut PPL cartridge (Agilent, Santa Clara, CA, USA) preconditioned

Fig. 1 Map of sampling points located at the Harney River, Everglades National Park

with one-cartridge volume of methanol followed by 2-cartridges-volume of water (pH 2). The loaded cartridge was then rinsed with water (pH 2) and dried with N₂ gas for 5 min prior to the elution of DOM molecules with 20 mL of methanol. SPE methanol extracts were stored in pre-washed glass vials at -20 °C. For comparison purposes, a dilution was used based on the estimated DOC content of the SPE extracts (less that 2× variation across samples). The purpose of the dilution is to have similar ionization and matrix effects across the transient samples. All samples were diluted to a final concentration of ~12 mg/l C in a 1:9 methanol: ethanol v:v solution mixture. All solvents used were of Optima LC-MS grade obtained from Fisher Scientific (Pittsburgh, PA, USA). Dissolved Organic Carbon (DOC) concentrations were analyzed at the NELAC-accredited CAChE Nutrient Analysis Core facility at Florida International University.

ESI-TIMS-FT ICR MS

A custom-built ESI-TIMS-FT-ICR MS platform based on a Solarix 7T FT-ICR MS equipped with an infinity ICR cell (Bruker Daltonics Inc., MA) was used for the experiments. An electrospray ionization source (Apollo II ESI design, Bruker Daltonics, Inc., MA) was utilized in negative ion mode and sample solutions were infused at 130 μ L/h. Typical operating conditions were 3200–3500 V capillary





voltage, 4 L/min dry gas flow rate, 1.0 bar nebulizer gas pressure, and a dry gas temperature 180°C. The instrument was optimized for high transmission of ions in the 100-1200 m/z range. Typical operational parameters included funnel rf amplitude 220 peak-to-peak voltage (Vpp), capillary exit - 100 V, deflector plate - 90 V, skimmer 1 - 60 V, transfer line rf 350 Vpp, octupole rf amplitude 350 Vpp and collision cell rf 1000 Vpp. Mass spectra were collected with a 4 MW data acquisition size for a mass resolution of ~300K at 400 m/z. Ions were accumulated for 20 s in the instrument collision cell before their transmission to the ICR cell. Experimental run time was about 3 hours using the FT-ICR MS serial mode. Solvent blanks were analyzed under the same experimental conditions as the samples and mass peaks detected in the blanks were removed from the samples mass lists. Agilent Tuning Mix calibration standard was used during the instrument tuning and control optimization.

The fundamentals on the gas phase ion TIMS separation and the coupling the FT-ICR MS can be found elsewhere (Tose et al. 2018; Benigni and Fernandez-Lima 2016; Benigni et al. 2017; Benigni et al. 2018). Briefly, an electric field is applied in the TIMS cell to hold ions stationary against a flowing gas, so that the drag force is evened with the electric field and ions are spatially separated across the TIMS analyzer axis based on their mobility (Fernandez-Lima et al. 2011a; Hernandez et al. 2014; Fernandez-Lima et al. 2011b). A quadrupolar field is also used during the gas phase separation to confine the ions radially, thus enhancing the trapping efficiency. The mobility, K_0 , of an ion in a TIMS cell is described by the Eq. (1):

$$K_0 = \frac{v_g}{E} = \frac{A}{V_{\text{elution}} - V_{\text{out}}},\tag{1}$$

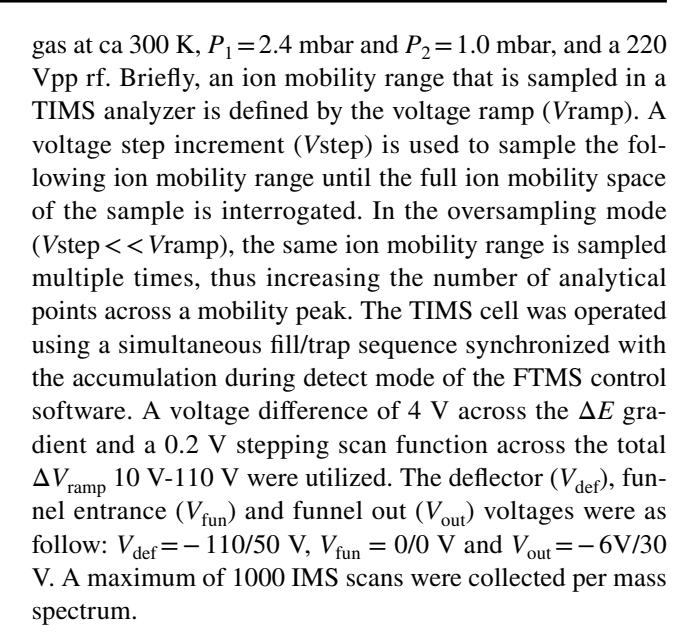
where $v_{\rm g}$, E, A, $V_{\rm elution}$, and $V_{\rm out}$ are the velocity of the gas, electric field, a calibration constant, elution voltage, and tunnel out voltage, respectively.

Values of K_0 can be converted into ion–neutral CCS (Ω , \mathring{A}^2) using the Mason–Schamp Eq. (2):

$$\Omega = \frac{(18\pi)^{1/2}z}{16(k_B T)^{1/2}} \left(\frac{1}{m_i} + \frac{1}{m_b}\right)^{1/2} \frac{1760T}{KoP273.15N^*},\tag{2}$$

where z is the charge of the ion, k_B is the Boltzmann constant, N^* is the number density, and m_i and m_b are the masses of the ion and bath gas, respectively(McDaniel and Mason 1973).

The TIMS analyzer was controlled using an in-house software, written in National Instruments LabVIEW, and synchronized with the FTMS control acquisition program. Ion mobility separation was conducted in the oversampling mode (Tose et al. 2018; Leyva et al. 2019; Leyva et al. 2020; Benigni and Fernandez-Lima 2016) using nitrogen as a bath



Data analysis

ESI-TIMS-FT-ICR MS data was processed using Data Analysis (v. 5.2, Bruker Daltonics, City, CA, USA). Chemical formula assignment was conducted using Composer software (version 1.0.6, Sierra Analytics, City, CA, USA) and confirmed with Data Analysis (version 5.2, Bruker Daltonics). Molecular formulas with the lowest errors, isolated assignments removal (de-assignment of peaks belonging to classes with only a few sparsely scattered members) and the presence of isotopologue signals were used as validation parameters. Theoretical formula constraints of $C_{4-50}H_{4-100}N_{0-3}O_{0-25}S_{0-2}$, S/N > 3, m/z range 100-650, error < 1 ppm and 0 < O/C < 1, 0.3 < H/C < 2.5, and DBE-O < 10 (Herzsprung et al. 2014) were considered. Near 50 mass peaks of predefined oxygen homologous series (O₃–O₁₀) compounds spaced approximately 14 mass units across the 200-600 m/z range were utilized for internal calibration in Composer. The walking internal recalibration resulted in an average error < 110 ppb for the mass range 200-600 Da. The TIMS spectra were externally calibrated for mobility using the Agilent Tuning Mix calibration standard (Stow et al. 2017). The number of isomers per chemical formula are estimated by deconvoluting (fitting gaussian peaks under the IMS profiles) the extracted ion mobiliograms of the assigned chemical formulas in the samples. This process was conducted using a custom-built Software Assisted Molecular Elucidation (SAME) written in Python v3.7.3. The SAME algorithm utilizes noise removal, mean gap filling, asymmetric least squares smoothing for base line correction, continuous wavelet transform (CWT)-based peak detection (SciPy package), and Gaussian fitting with non-linear least squares functions (Levenberg-Marquardt algorithm) (Benigni et al. 2017). Plots were created using



Microsoft Excel 365, OriginPro 2016 (Originlab Co., MA), and Python 3.7.3. To compare the molecular signatures of DOM along the transect, isomeric weighted averages of specific molar ratios (H/C, O/C, #N), modified aromatic index (AI_{mod}) were calculated for all samples based on the number of isomers assigned to each molecular formula using a similar approach as the ones previously reported (Seidel et al. 2014; Koch and Dittmar 2006). Chemical formulas identified across DOM samples were tagged with their underlying isomeric information (TIMSCCS_{N2} values). A comparison of the chemical formulas-TIMSCCS_{N2} across DOM samples considering an 8% matching error on TIMSCCS_{N2} values was conducted using mathematical sets in Python 3.7.3.

Results and discussion

The ESI(-)-TIMS- FT ICR MS analysis of the five SPE-DOM samples collected along the salinity transect of the Harney River estuary resulted in the typical single, broad trend line of [M–H]⁻ molecular species ($1/K_0$ range: 0.6-1.2 Vs/cm²) in the 2D IMS-MS domain (Fig. 2A). Overall, a Gaussian-like MS distributions across 190–650 m/z with the apex centered at ~370 m/z were found for all samples (See Fig. 2A insets). Interestingly, a slightly different profile depleted in mass signals over $400 \, m/z$ was found for the sample HR-4, which may suggest a change in the compositional nature of this sample.

Around 70% of the chemical formulas detected at the freshwater marsh station were identified at the marine endmember. This decreasing trend in molecular diversity resonates with a declining pattern of CDOM (UV absorbance, 254 nm) previously observed in the same system (Cawley et al. 2014). The change in DOM molecular diversity perceived along the Harney River could be partially explained by the fact that much of the DOM in the upper headwaters of the Harney River is derived from the Everglades freshwater marshes. This freshwater signal is reduced along the salinity transect through biogeochemical processing including bio- and photo- degradation, while a smaller but significant amount of DOM components is added from the mangrove marsh and the marine end member (Cawley et al. 2014). Other studies (Seidel et al. 2015; Sleighter and Hatcher 2008) have reported similar trends for more geographically extensive watersheds (compared to this study) and suggested this pattern to be driven by the river continuum concept (RCC), where low stream orders (headwaters) feature more chemically complex DOM than high stream orders (estuary) since more labile DOM components may degrade downstream (Creed et al. 2015; Vannote et al. 1980). In agreement with the literature, the difference in molecular diversity observed at the station HR-5 (1625 formulas) compared to HR-4 (1373 formulas), suggests a potential

Table 1 Summary of the isomeric information obtained for the Harney River DOM samples using TIMS-FT-ICR MS

Parameter	Sample ID				
	HR-1	HR-2	HR-3	HR-4	HR-5
m/z_w	414.36	406.47	396	379.23	378.23
C_w	18.56	19.47	18.84	18.15	17.89
N_w	0.35	0.42	0.41	0.42	0.39
O_w	10.09	8.57	8.38	7.92	7.97
S_w	0.24	0.22	0.26	0.23	0.3
H/C_w	1.00	1.21	1.22	1.24	1.23
O/C_w	0.55	0.45	0.46	0.45	0.46
N/C_w	0.02	0.03	0.03	0.03	0.03
S/C_w	0.02	0.01	0.02	0.02	0.02
DBE_{w}	10.51	8.99	8.61	8.16	8.1
$AImod_w$	0.143	0.115	0.107	0.106	0.11
Total isomers	22,185	18,236	12,549	10,414	13,256
CHO isomers	11,783	11,027	7591	6817	7475
CHO isomers%	53.1	60.5	60.5	65.5	56.4
CHON isomers	5109	3127	1733	1228	1848
CHON isomers%	23.0	17.1	13.8	11.8	13.9
CHOS isomers	5293	2981	2359	1527	3206
CHOS isomers%	23.9	16.3	18.8	14.7	24.2
CHONS isomers	0	1101	866	842	727
CHONS isomers%	0.0	6.0	6.9	8.1	5.5

contribution of mangrove and marine-derived DOM at the marine endmember.

An increase in unsaturation of higher molecular mass and size DOM components was clearly observed (Fig. 2B). The decrease in the number of compounds with higher m/zand DBE values observed along the salinity gradient suggests that highly unsaturated DOM components are mainly derived from the Everglades freshwater marsh environment and are preferentially transformed during their transport from land to sea. A detailed inspection of Table 1 confirmed a decrease of DBE_w and an increase in the H/C_w along the transect. Previous reports have concluded that unsaturated aromatic DOM compounds are favorably bleached during the photodegradation of DOM samples from fresh/brackish waters (Sleighter and Hatcher 2008; Kujawinski et al. 2004; Minor et al. 2007; Dalzell et al. 2009; Wilske et al. 2020; Gonsior et al. 2009). Furthermore, it has been found that molecular species resulting from photodegraded freshwater DOM resembled the composition of higher salinity samples (Minor et al. 2007; Stubbins et al. 2010). A closer view at the van Krevelen plots in Fig. 2C evidenced that the removal of unsaturated, tannins-like compounds at the freshwater endmember significantly contributed to the overall decreasing trend observed in aromaticity and degree of unsaturation along the transect. These findings suggest that



53 Page 6 of 14 D. Leyva et al.

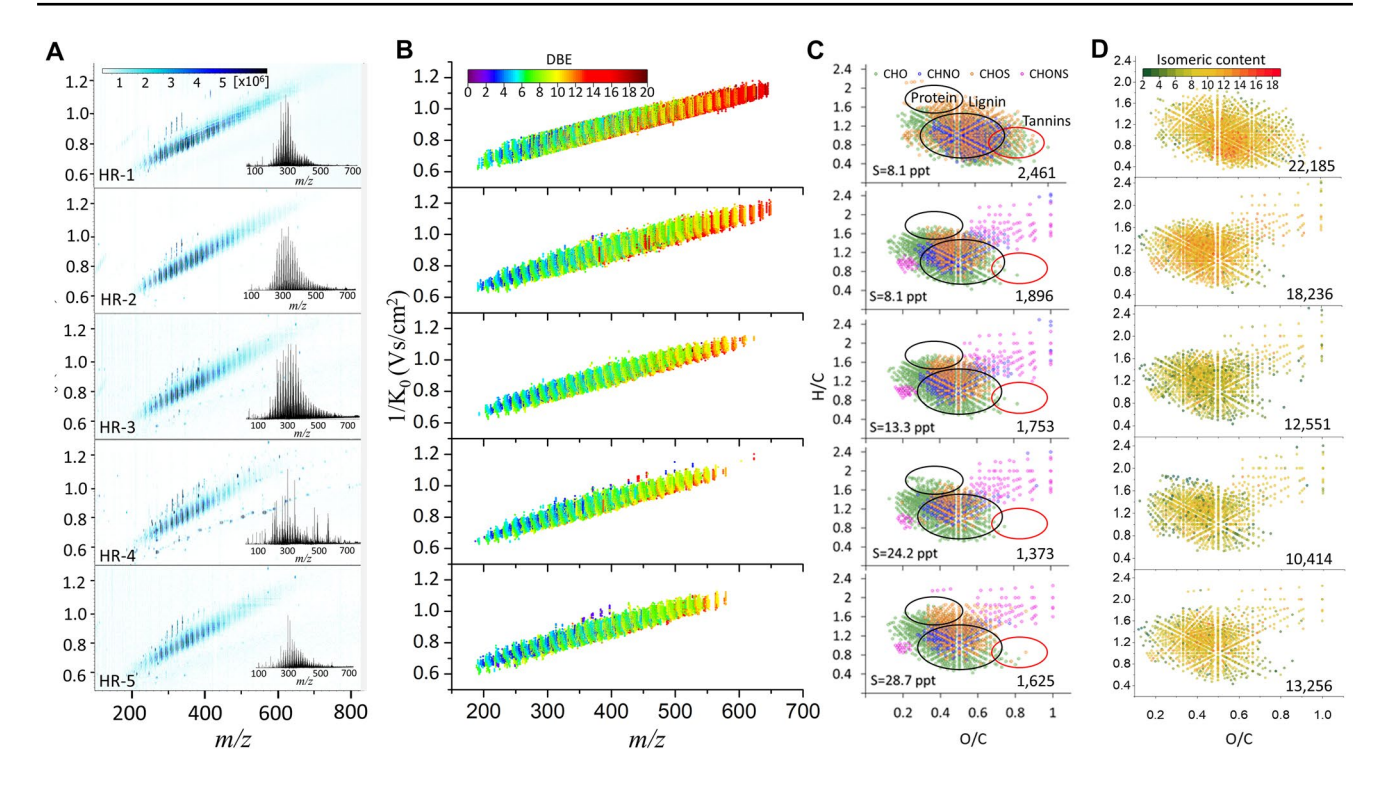


Fig. 2 2D IMS-MS profiles of Harney River SPE-DOM samples obtained from ESI-TIMS-FT ICR MS (A). Broadband MS¹ projections shown as insets. 2D IMS-MS profiles including DBE distribution of molecular formulas assigned in each sample. Note the consistent decrease of highly unsaturated molecules (red color) along the transect (B). Van Krevelen plots of the assigned molecular spe-

cies (chemical classes indicated by colors) denoting a change in the molecular complexity of the samples as a function of the salinity (S). Van Krevelen plots indicating a decrease in the isomeric content from freshwater DOM to the estuary influenced DOM (D) (colour figure online)

photodegradation plays a crucial role during DOM transport and mineralization in the Harney River.

The projection of the elemental ratios in the compositional space revealed a set of core molecules in the lignintype area of the van Krevelen plot that remained unaltered along the salinity transect (See Fig. 2 C). Previous studies using optical properties, in particular EEM PARAFAC, have shown that while some components increased or decreased along the salinity gradient (suggesting additional contributions from the mangrove marshes and seagrass, and DOM removal resulting from degradation processes), one PARA-FAC component remained unaltered showing high resistance to degradation and a conservative mixing behavior along the salinity transect (Cawley et al. 2014). The unaltered and seemingly resistant isomers observed in this study may be related to this PARAFAC component. These DOM components have been previously associated with a constrained set of terrestrial recalcitrant material (e.g. aliphatic and carboxylic-rich alicyclic molecules) that partially resist degradation(Stubbins et al. 2010). However, a visual inspection of the plots in Fig. 2 C indicates that an important set of CHO, CHON, and CHOS molecular species change significantly from the freshwater marshes to the estuary. A detailed analysis of Table 1 confirmed an overall decrease in the number of compounds for all the heteroatom classes along the transect. Interestingly, while heteroatom components are clearly bio- or photo-degraded along the salinity gradient, the enriched molecular complexity observed at the lower estuary (site HR-5) compared with HR-4 is primarily attributed to an increase in CHON (~30%) and CHOS (~50%) molecular formulas. The source for these heteroatomic components at higher salinity is usually associated with DOM inputs from the mangrove swamps and/or marine vegetation, or biogeochemical transformations of DOM components transported along the transect. (Seidel et al. 2014, 2015; Sleighter and Hatcher 2008; Osterholz et al. 2016b) Although there is no documented ultrahigh-resolution mass spectrometry analysis of the Harney River DOM, a previous report based on optical properties and stable isotopes found significant contributions of seagrass DOM to the pool of DOC in several regions of Florida Bay(Ya et al. 2015), and a biomarker-based study of sediments in the Harney River estuary reported on seagrass as a potential source of sedimentary organic matter in the estuary (Jaffé et al. 2001). A molecular-level analysis of DOM performed at a terrestrialsalinity transect in Elizabeth River, Virginia, correlated the significant input of CHON and CHONS molecular species at the estuary with a source of primary producers(Sleighter



and Hatcher 2008). In contrast, the enrichment of CHOS components to the DOM signature at the mangrove-estuary region has not been clearly elucidated(Wagner et al. 2015; Sleighter and Hatcher 2008).

A decreasing pattern, analogous to the one observed for molecular formulas, was found for the estimated number of isomers along the salinity transect (Fig. 3). Nearly twofifth of the isomers detected at the freshwater end-member were not found above the signal-to-noise ratio defined or transformed downstream, in contrast with a freshwater-toestuarine isomeric complexity enrichment in a salinity gradient in a tributary channel of the Mississippi River (based on isomeric distinctive cluster percentage reported from IM Q-TOF LC/MS by Lu et al. (2021). Overall, the spike in isomeric complexity (over 3000 new isomers) observed at the downstream-most estuarine site (station HR-5) was highly influenced by CHON and CHOS compound classes (Table 1). These results suggest that the spatial variability observed in DOM isomeric complexity along the Harney River may be highly influenced by the input from mangroves and potentially seagrass. Reports from Schmidt et al. (2009) and Powers et al. (2021) have suggested that sulfurization processes may contribute to the characteristic compositional signature of porewater DOM in coastal areas. Interestingly, lignin-like components hold the highest isomeric complexity across the samples with an average of 10–12 isomers per molecular formula (See Fig. 2D).

The Venn diagram depicted in Fig. 3 shows that near 800 molecular features were shared by all DOM transect samples suggesting that a group of terrestrial-derived components persisted unaltered along the Harney River. On the other hand, molecular formulas were also found to be unique to each section of the transect. While the total number of molecular formulas decreases along the salinity transect, a slight increase was found at the marine endmember compared to the sampling points at intermediate salinity. This result agrees with previous findings on the contribution of

marine-derived components to the pool of DOM molecules in the Harney River.

Inspection of the DOM composition based on unique and common molecular formulas across the transect as a function of DBE (Fig. S1) reveals the removal of highly unsaturated components from the freshwater endmember. These results confirmed previous findings of the significant export of saturated refractory lignin-type DOM components in coastal ecosystems (Koch et al. 2005; Sleighter and Hatcher 2008). A closer view of the van Krevelen plots of molecular formulas shared by all samples (Fig. S2A) shows an enrichment in DOM isomeric complexity at the segment HR-1 to HR-2, followed by a pattern that exhibits a less complex DOM until the river estuary. The same analysis extended to heteroatom classes (Fig. S2B-D) indicated that CHO species were the main contributor to the surge in isomeric complexity at the sampling point HR-2. Since salinity at the upper estuary (e.g. HR-2) is usually higher during the dry season when freshwater discharge into the estuary is lower, DOM is exposed to higher phosphorus conditions in this 'upside down' estuary (Childers et al. 2006), and thus to different microbial conditions under less nutrient limitations. This fact might enhance degradation of DOM components that were more refractory under freshwater conditions.

Over 1100 distinctive molecular formulas, with mostly tannins-like characteristics, were identified at the freshwater sample (See van Krevelen plot of Unique HR-1 in Fig. 3). Plant-derived material exported to freshwater has been recognized as the main source of the DOM signature observed at the Everglades coastal wetlands (Hertkorn et al. 2016; Wagner et al. 2015; Maie et al. 2005). In comparison to the molecular signature of unique components detected at HR-1, the mid-salinity sampling points in the mangrove estuary revealed a major removal of tannins-like species derived from the freshwater endmember. Reports from incubation experiments have attributed the sink of such aromatic tannins-like species to several biogeochemical processes

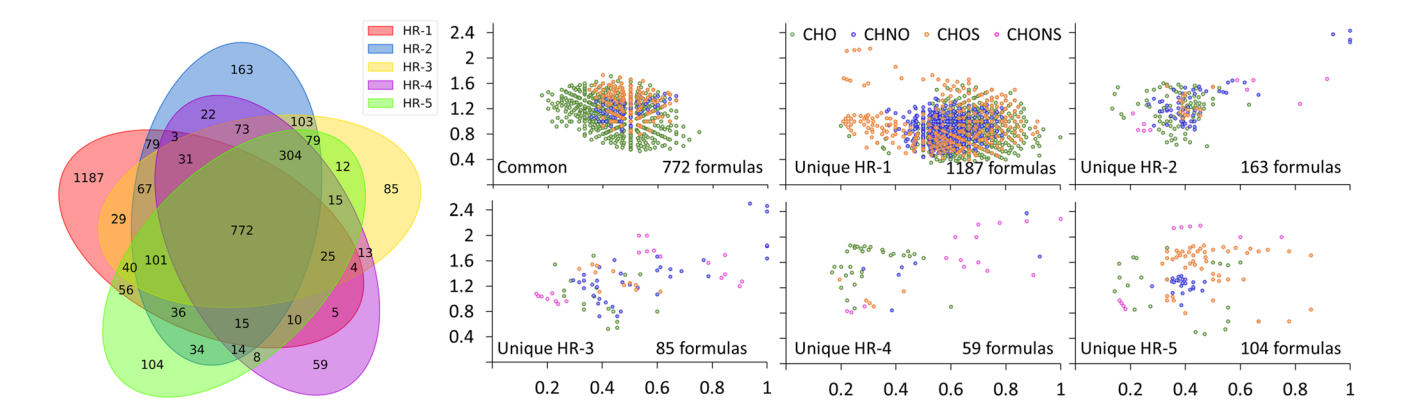


Fig. 3 Venn diagram indicating the common and unique molecular species identified by ESI-FT-ICR MS across the salinity transect (left). Van Krevelen plots of common and site-specific DOM molecular species (right)



including biodegradation (Ward et al. 2013) and photo mineralization (Gonsior et al. 2009; Stubbins et al. 2010; Ward and Cory 2016). Nevertheless, other potential mechanisms such as co-precipitation (Maie et al. 2008), flocculation (Asmala et al. 2016), sorption (Groeneveld et al. 2020), dilution (Medeiros et al. 2015), and non-conservative mixing are very likely to also influence the observed compositional changes.

Unique CHNO and CHOS molecular species were also detected at the freshwater end member (See Fig. 3). Previous works have suggested that sulphate contributions from different sources (agriculture, sea spray, etc.) may contribute to the CHOS signature of DOM at the Everglades wetlands (Hertkorn et al. 2016; Wagner et al. 2015).

Few unique DOM molecular species were found across samples HR-2 to HR-5 compared to HR-1, indicating that the compositional fingerprint of DOM exported to the ocean is highly dominated by the molecular signature of marsh derived DOM from the freshwater endmember. However, a minor input of unique molecular compounds observed downstream is a clear indication of the contribution of the Everglades mangrove forest and seagrass to the estuary DOM. Although this is the first report on the molecular level characterization of DOM along the Harney River, previous studies of carbon dynamics in the same area utilizing optical properties (Cawley et al. 2014; Regier and Jaffé 2016) have suggested up to 20% DOC contributions from the fringe mangrove system. In agreement with our results, a comparative study of DOM dynamics in three coastal wetland systems across the world, using optical properties, has found some mangrove-derived DOM material at regions of intermediate salinities in the Harney River that are equivalent to our sampling points HR-2 and HR-3 (Maie et al. 2014).

Interestingly, a set of common compounds to samples HR-2-HR-5, mainly CHO and CHNOS, was found, indicating an export of lignin-like refractory DOM from the mangrove forests and/or the formation of degradation products from the freshwater endmember along the salinity gradient (Fig. S3). In a recent study (Harir et al. 2022), sequential photo degradation and photo generation of CHNO and CHOS compounds were observed during a light exposed time series of freshwater DOM from the Everglades. The exact source and environmental dynamics of CHNOS DOM compounds could not be clearly determined in this study. Nevertheless, the distribution of the two CHNOS compound clusters in the compositional space (Fig. S3) indicates that the reduced (O/C < 0.4) and relatively unsaturated species and the oxidized (O/C > 0.8) aliphatic material might be possibly associated with sulfur containing protein degradation products (Osterholz et al. 2016a; Seidel et al. 2014, 2015; Sleighter and Hatcher 2008) given the high diversity in reaction pathways of DOM N-bearing components in the estuary-marine interface (Schmidt et al. 2011).

The ESI-TIMS-FT-ICR MS analysis provided ion mobility information at the chemical formulae level. Each isomer can be characterized by its TIMSCCS_{N2}, which is an indication of the size and shape of the chemical structure. For example, a long aliphatic chain structure exhibits larger TIMSCCS_{N2} values than a more compact isomeric structure. The addition of the isomeric dimension, based on TIMSCCS_{N2}, to each chemical formula reveals a novel layer of structural information which is invisible in the mass domain. The chemical formulas assigned to each DOM sample were tagged with their corresponding isomeric information (TIMSCCS_{N2} values). A further comparison of concatenated chemical formulas with their TIMSCCS_{N2} values was conducted across DOM samples for the identification of characteristic and common isomeric species along the transect. Over 4,000 structural isomers linked to 772 molecular formulas shared by the five DOM samples were transported from the freshwater end member to the sea (See Venn diagram in Fig. 4). In another study, a structural analysis based on CID fragmentation of selected DOM precursor molecules in the geographically much more extensive Delaware estuary found no significant differences among DOM structural features of molecular formulas common to all samples collected along a salinity gradient (Osterholz et al. 2016a). The authors suggest that these consistent DOM features along the salinity gradient could be the result of a high degree of recalcitrance of the terrestrial endmember DOM, resulting in negligible biogeochemical degradation, or that while some of the DOM components are actually removed during transport, similar compounds are produced at the same time, as previously suggested by Sleighter and Hatcher (Sleighter and Hatcher 2008). In contrast, while our results suggested a major change in the DOM isomeric pool along the salinity transect (only ~20% of the total number of isomers detected at the freshwater end member were presumably transported downstream), an analogous reasoning as the one utilized by Osterholz et al. (2016b) in the molecular formula domain could be extended here at the isomeric level. Thus, we hypothesize that while dilution and degradation processes may lead to a potential depletion of some isomeric species during their transport from land to sea, the input at higher salinities of isomers derived from fringe mangrove and marine end member sources share close structural similarities to the terrestrial derived compounds found upstream (i.e., $^{TIMS}CCS_{N2}$ values within 8%Å²). Such process could function as an apparent "isomeric replacement". This information, obtained for the first time at a complex aquatic ecosystem, provides new insights into the isomeric nature of DOM components. Yet, further studies are needed to clearly understand the role of input sources on shaping the isomeric signature of DOM and the potential structural features that contribute to the long-term stability of refractory DOM components.



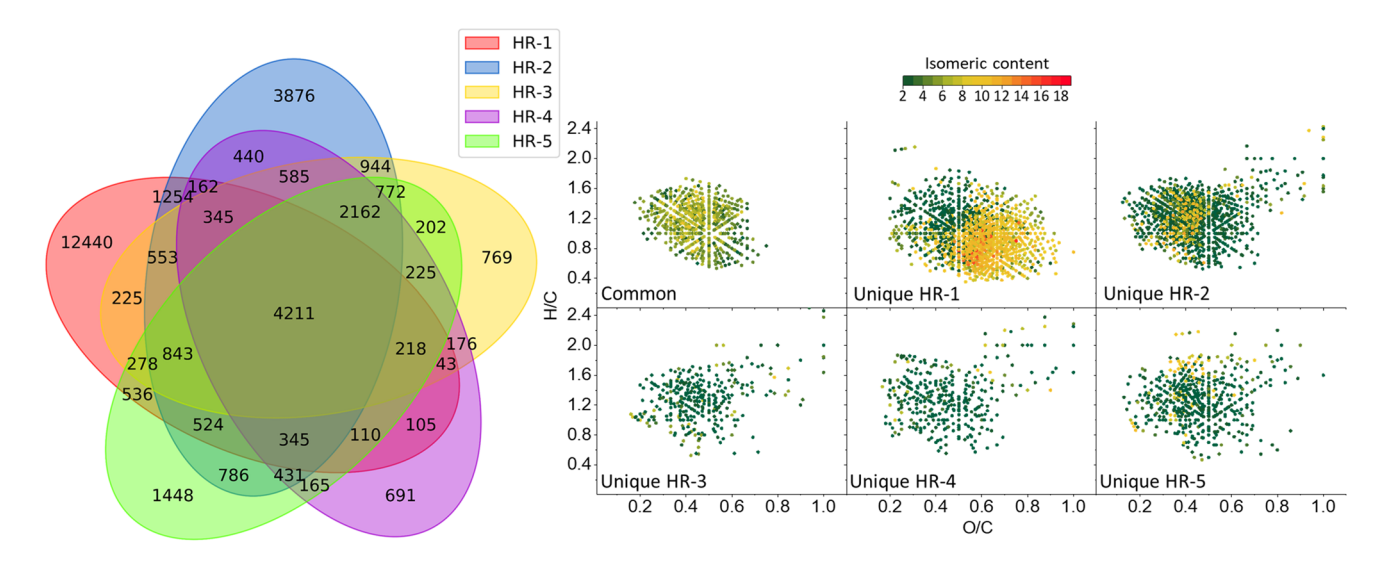


Fig. 4 Venn diagram indicating the common and unique isomeric species filtered by their $^{\text{TIMS}}\text{CCS}_{\text{N2}}$ values determined from ESI-TIMS-FT-ICR MS with a threshold error of <8% (left panel). The

van Krevelen plots of common and unique isomers with the number of isomers plotted as a third dimension (right panel)

The number of isomeric compounds unique to each DOM sample along the estuarine transect, filtered based on both chemical formula and TIMSCCS_{N2} values, showed a declining profile in the order HR-1 > HR-2 > HR-5 > HR-3 > HR-4. This trend resembles the one obtained for the site-specific chemical formulas (See Venn diagram of Fig. 3). However, some slight differences can be highlighted here. First, a highly diverse isomeric content attributed to the sample HR-1 (> 12,000 unique structural isomers detected) clearly shows that degradation along the transect may have a major impact on DOM isomeric diversity. Second, the increased isomeric complexity found at HR-5 compared to the nearest upstream sites (HR-3 and HR-4), suggests a preferential input of isomeric components presumably from primary production at the marine end member.

The van Krevelen plots of common DOM isomers found across the transect (Fig. 4) suggests that the main contribution to the isomeric diversity of DOM exported from the Everglades to the coastal system is preferentially derived from lignin-like species originated at the freshwater endmember (average of 6 isomers per chemical formula). Noteworthy, two isomeric diverse clusters can be distinguished from the van Krevelen diagram at sample points HR-1 and HR-5. In the first case, highly structurally complex tanninlike molecules observed at HR-1 support our previous findings that the structural diversity of these particular components is substantially reduced though downstream estuarine biogeochemical processes. On the other hand, the proteinlike signature detected at HR-5 with an average of 6–8 isomers per chemical formula (yellow dots in the van Krevelen plot) clearly suggests DOM contributions of more isomeric complex mangrove and/or marine derived DOM. The unique and common isomeric species identified by ESI-TIMS-FT-ICR MS across the samples in this study could be further explored as potential chemo-markers to fingerprinting natural sources of DOM in this coastal ecosystem.

Heatmaps highlighting the total isomeric content of the chemical formulas (indicated in parenthesis) common to all sites as a function of DBE, oxygen class and salinity are described in Fig. 5. The analysis of the isomeric content along the transect (horizontal trend) as a function of the oxygen class revealed a decreasing profile in the isomeric diversity with increasing salinity for relatively poor oxygenated isomers (up to 6 oxygens). On the contrary, more oxygenated species exhibited a varying isomeric pattern along the transect with and initial apparent isomeric enrichments at the second lowest salinity site HR-2, followed by a decreasing isomeric enrichment until a second enrichment at the highest salinity site HR-5 (see O7-O10 profiles). The observed relative increase in the isomeric content observed at HR-2 and HR-5 could be associated with the input of isomers resulting from early degradation processes occurring in the upper estuary, when phosphorus limitations are first reduced, followed by isomeric inputs derived from mangrove and marine derived DOM observed at HR-5. A closer view at the Fig. 5 shows that the isomeric diversity of more unsaturated compounds (7 \leq DBE \leq 10) changed with increasing salinity regardless of the chemical formula diversity and the oxygen class. In contrast, the more aliphatic structural isomers (DBE < 6), showed a higher resistance to molecular transformations. Note that since we are considering the sum of estimated isomers for all chemical formulas of the same O-class and DBE, other trends at the chemical formula level may not be uncovered.



53 Page 10 of 14 D. Leyva et al.

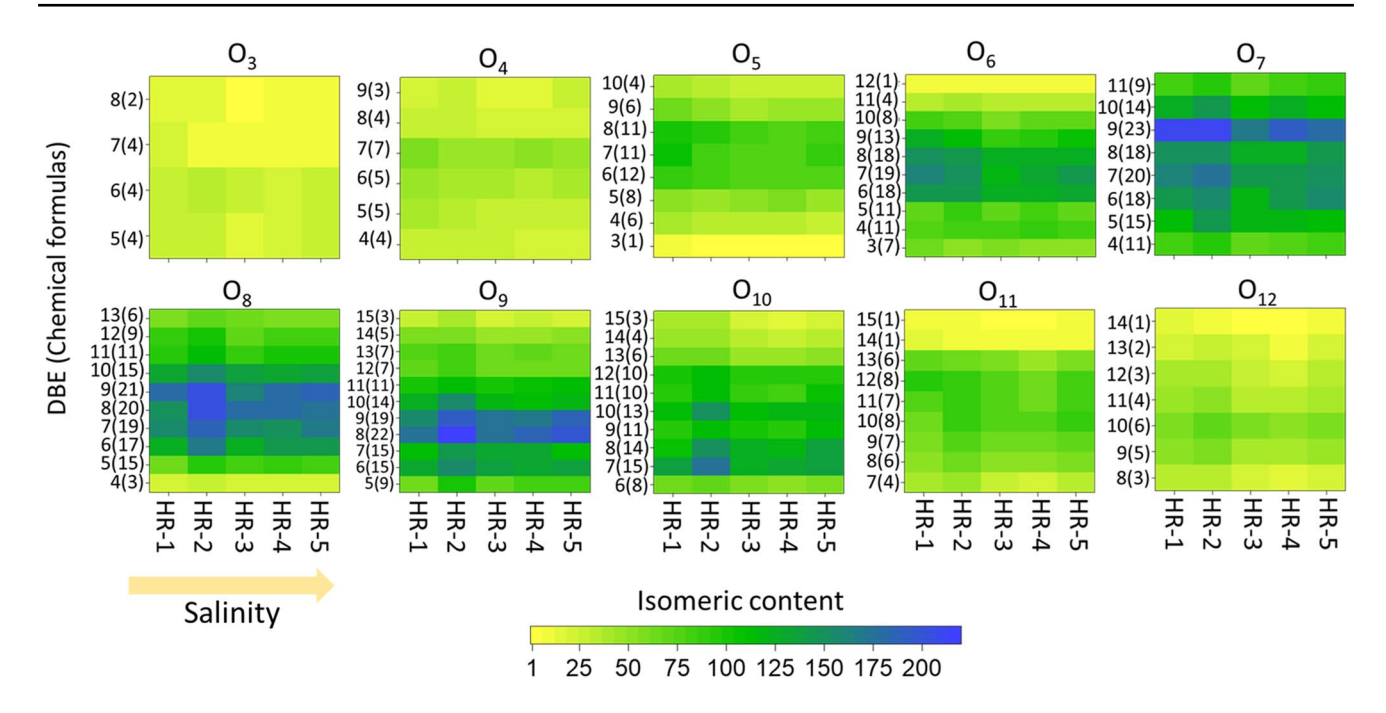


Fig. 5 Contour plots showing the distribution of the isomeric diversity from chemical formulas common to all sites as a function of DBE, oxygen class and salinity. Note that each box in the contour

plot included the sum of the estimated number of isomers for all the chemical formulas sharing the same DBE (number in parenthesis)

The inspection of the isomeric information at the level of DOM chemical formulas can illustrate previous observed trends across the salinity transect of the Harney River (Fig. S4, see example for $C_{14}H_{10}O_7$ and $C_{15}H_{14}O_6$). In the examples shown, the number of isomers across the salinity transect correlates with the transformation trends described before (see Fig. 5). That is, the higher oxygenated and higher DBE C₁₄H₁₀O₇ strongly varies in isomeric diversity (decreased from 12 to 5 minimum isomers along the transient), suggesting that higher oxidized and more unsaturated isomeric species are more prone to biogeochemical transformations. In contrast, other molecular species with lower oxygenation and DBE C₁₅H₁₄O₆ showed no variation in the number of potential isomers along the transient. Although our results seem to contrast with the degradation patterns as a function of salinity observed by Osterholz et al. (2016a) for less oxygenated polyphenol chemical formulas $(0.5 < AImod \le 0.66)$, critical differences in both approaches need to be highlighted. While Osterholz's data involved normalized abundances of chemical formulas assigned from FT-ICR MS signals, our approach rests on estimated number of isomers obtained by ion mobility spectrometry. Nevertheless, changes in the relative abundance across the isomers per chemical formula observed along the transect best reflect the isomeric chemical diversity with salinity. While only a small number of isomers are accounted for in this analysis, other isomeric trends could be present and not accessible based on differences in mobility per chemical formula.

Further, more in depth studies in this field are warranted to uncover additional information that isomeric data can provide to better understand biogeochemical cycling of DOM.

Conclusion

A characterization of DOM isomeric complexity using ESI-TIMS-FT ICR MS was conducted for the first time along a freshwater marsh fed mangrove estuary salinity transect (the Harney River in the Florida Everglades). Overall, while the number of detected DOM molecular formulas decreased with increasing salinity, the compositional signature of DOM varied from more unsaturated and oxygenated to more aliphatic and heteroatom diverse components along the transect. While the estimated number of isomeric DOM compounds consistently declined downstream, a relatively small set of terrestrial-derived DOM components remained structurally unchanged (isomers with $\Delta^{\hat{TIMS}}CCS_{N2}$ values < 8%). Our results provide novel evidence of the increase in refractory character for DOM isomeric species as both DBE and oxygenation decreases, contrasting with unchanged isomeric patterns detected along a similar freshwater-to-estuarine system (Osterholz et al. 2016a). A detailed examination of unique molecular components to each sample evidenced that DOM chemical fingerprint in this estuary is highly influenced by multiple input sources from different origins including the freshwater marsh, mangrove, and primary producers. Nevertheless, several biogeochemical degradation



and transformation processes are also likely involved in the modulation of DOM isomeric molecular fingerprint along the transect. Though previous works using traditional and optical techniques (i.e., DOC and fluorescence) have provided valuable information of bulk DOM change along the Harney River freshwater-to-marine system, our results constitute the first view of DOM variability at the isomeric level. The analysis of ion mobility data from molecular formulas unique to each sample indicates that terrestrial, freshwater marsh-derived material is up to four times more isomeric complex than marine primary producers and mangrove DOM. The inspection of the isomeric information at the level of DOM chemical formulas revealed that higher oxidized and more unsaturated isomeric species are more prone to biogeochemical transformations. Moreover, the unique molecular features identified across all the samples in this study, along with their specific isomeric characteristics may be used as potential chemo-markers that can help to better elucidate the linkage between DOM molecular fingerprint and input sources and/or related biogeochemical processing during transport. Our findings on tracking the changes in chemical and isomeric signatures of DOM along coastal gradients illustrate that ESI-TIMS-FT-ICR MS is a useful tool that will help to expand the current knowledge of the carbon fate in coastal aquatic ecosystems.

Supplementary Information The online version contains supplementary material available at https://doi.org/10.1007/s00027-022-00887-y.

Acknowledgements This work was supported by the National Science Foundation Division of Chemistry, under CAREER award CHE-1654274, with co-funding from the Division of Molecular and Cellular Biosciences to FFL. DL acknowledges the fellowship provided by the National Science Foundation award (HRD-1547798) to Florida International University as part of the Centers for Research Excellence in Science and Technology (CREST) Program. DL also would like to acknowledge Edward Castañeda, and Ryan Bremen and Kenny Anderson from the Ecosystem Ecology Laboratory at Florida International University (FIU) for their field and laboratory support, as well as Michael G Rugge from the Institute of Environment at FIU for his help on generating the map. This is contribution number xxxx from the Institute of Environment at Florida International University. This material was developed in collaboration with the Florida Coastal Everglades Long Term Ecological Research program under National Science Foundation Grant No. DEB-2025954. The authors acknowledge the personnel of the Advance Mass Spectrometry Facility at Florida International University as well as David Stranz and Sierra Analytics, Inc. for their support with the Composer software.

Author contributions The manuscript was written through contributions of all authors. All authors have given approval to the final version of the manuscript.

Data availability The TIMS-FT-ICR MS raw data from the SPE-DOM samples is freely accessible at https://doi.org/10.34703/gzx1-9v95/ZW5RIM.

Declarations

Conflict of interest The authors declare no competing interests.

References

- Asmala E, Kaartokallio H, Carstensen J, Thomas DN (2016) Variation in Riverine Inputs Affect Dissolved Organic Matter Characteristics throughout the Estuarine Gradient. Front Mar Sci 2:1–15. https://doi.org/10.3389/fmars.2015.00125
- Asmala E, Massicotte P, Carstensen J (2021) Identification of dissolved organic matter size components in freshwater and marine environments. Limnol Oceanogr 66:1381–1393. https://doi.org/10.1002/lno.11692
- Benigni P, Fernandez-Lima F (2016) Oversampling Selective Accumulation Trapped Ion Mobility Spectrometry Coupled to FT-ICR MS: Fundamentals and Applications. Anal Chem 88:7404–7412. https://doi.org/10.1021/acs.analchem.6b01946
- Benigni P, Thompson CJ, Ridgeway ME, Park MA, Fernandez-Lima F (2015) Targeted High-Resolution Ion Mobility Separation Coupled to Ultrahigh-Resolution Mass Spectrometry of Endocrine Disruptors in Complex Mixtures. Anal Chem 87:4321–4325. https://doi.org/10.1021/ac504866v
- Benigni P, Marin R, Sandoval K, Gardinali P, Fernandez-Lima F (2017) Chemical Analysis of Water-accommodated Fractions of Crude Oil Spills Using TIMS-FT-ICR MS. J Vis Exp 121:e55352.
- Benigni P, Porter J, Ridgeway ME, Park MA, Fernandez-Lima F (2018) Increasing Analytical Separation and Duty Cycle with Nonlinear Analytical Mobility Scan Functions in TIMS-FT-ICR MS. Anal Chem 90:2446–2450.
- Berg SM, Peterson BD, Mcmahon KD, Remucal CK (2022) Spatialand temporal variability of dissolved organic matter molecular composition in astratified Eutrophic Lake. J Geophys Res 127:1–16. https://doi.org/10.1029/2021JG006550
- Buffam I, Turner MG, Desai AR, Hanson PC, Rusak JA, Lottig NR, Stanley EH, Carpenter SR (2011) Integrating aquatic and terrestrial components to construct a complete carbon budget for a north temperate lake district. Glob Change Biol 17:1193–1211. https:// doi.org/10.1111/j.1365-2486.2010.02313.x
- Cawley KM, Yamashita Y, Maie N, Jaffé R (2014) Using Optical Properties to Quantify Fringe Mangrove Inputs to the Dissolved Organic Matter (DOM) Pool in a Subtropical Estuary. Estuaries Coasts 37:399–410. https://doi.org/10.1007/s12237-013-9681-5
- Chen M, Maie N, Parish K, Jaffé R (2013) Spatial and temporal variability of dissolved organic matter quantity and composition in an oligotrophic subtropical coastal wetland. Biogeochemistry 115:167–183. https://doi.org/10.1007/s10533-013-9826-4
- Childers DL, Boyer JN, Davis SE, Madden CJ, Rudnick DT, Sklar FH (2006) Relating precipitation and water management to nutrient concentrations in the oligotrophic "upside-down" estuaries of the Florida Everglades. Limnol Oceanography 51: 602–616. https://doi.org/10.4319/lo.2006.51.1_part_2.0602
- Chow AT, Dai J, Conner WH, Hitchcock DR, Wang J-J (2013) Dissolved organic matter and nutrient dynamics of a coastal freshwater forested wetland in Winyah Bay, South Carolina. Biogeochemistry 112:571–587. https://doi.org/10.1007/s10533-012-9750-z
- Clark MG, Biagi KM, Carey SK (2022) Optical properties of dissolved organic matter highlight peatland-like properties in a constructed wetland. Sci Total Environ 802:1–13. https://doi.org/10.1016/j. scitotenv.2021.149770
- Creed IF, Mcknight DM, Pellerin BA, Green MB, Bergamaschi BA, Aiken GR, Burns DA, Findlay SEG, Shanley JB, Striegl RG,



- Aulenbach BT, Clow DW, Laudon H, Mcglynn BL, Mcguire KJ, Smith RA, Stackpoole SM (2015) The river as a chemostat: fresh perspectives on dissolved organic matter flowing down the river continuum. Can J Fish Aquat Sci 72:1272–1285. https://doi.org/10.1139/cifas-2014-0400
- Dalzell BJ, Minor EC, Mopper KM (2009) Photodegradation of estuarine dissolved organic matter: a multi-method assessment of DOM transformation. Org Geochem 40:243–257. https://doi.org/10.1016/j.orggeochem.2008.10.003
- Dittmar T, Koch B, Hertkorn N, Kattner G (2008) A simple and efficient method for the solid-phase extraction of dissolved organic matter (SPE-DOM) from seawater. Limnol Oceanography: Methods 6:230–235. https://doi.org/10.4319/lom.2008.6.230
- Fellman JB, Hood E, Spencer RGM (2010) Fluorescence spectroscopy opens new windows into dissolved organic matter dynamics in freshwater ecosystems: a review. Limnol Oceanogr 55:2452–2462. https://doi.org/10.4319/lo.2010.55.6.2452
- Fernandez-Lima FA, Becker C, Mckenna AM, Rodgers RP, Marshall AG, Russell DH (2009) Petroleum Crude Oil Characterization by IMS-MS and FTICR MS. Anal Chem 81:9941–9947. https://doi.org/10.1021/ac901594f
- Fernandez-Lima F, Kaplan DA, Suetering J, Park MA (2011a) Gasphase separation using a trapped ion mobility spectrometer. Int J Ion Mobil Spectrom 14:93–98. https://doi.org/10.1007/s12127-011-0067-8
- Fernandez-Lima FA, Kaplan DA, Park MA (2011b) Note: Integration of trapped ion mobility spectrometry with mass spectrometry. Rev Sci Instrum 82:126106. https://doi.org/10.1063/1.3665933
- Gao Y, Wang W, He C, Fang Z, Zhang Y, Shi Q (2019) Fractionation and molecular characterization of natural organic matter (NOM) by solid-phase extraction followed by FT-ICR MS and ion mobility MS. Anal Bioanal Chem. https://doi.org/10.1007/s00216-019-01943-7
- Gonçalves-Araujo R, Stedmon CA, Heim B, Dubinenkov I, Kraberg A, Moiseev D, Bracher A (2015) From Fresh to Marine Waters: Characterization and Fate of Dissolved Organic Matter in the Lena River Delta Region, Siberia. Front Mar Sci 2:1–13. https://doi.org/10.3389/fmars.2015.00108
- Gonçalves-Araujo R, Granskog MA, Bracher A, Azetsu-Scott K, Dodd PA, Stedmon CA (2016) Using fluorescent dissolved organic matter to trace and distinguish the origin of Arctic surface waters. Sci Rep 6:33978. https://doi.org/10.1038/srep33978
- Gonsior M, Peake BM, Cooper WT, Podgorski D, D'andrilli J, Cooper WJ (2009) Photochemically Induced Changes in Dissolved Organic Matter Identified by Ultrahigh Resolution Fourier Transform Ion Cyclotron Resonance Mass Spectrometry. Environ Sci Technol 43:698–703.
- Groeneveld M, Catalán N, Attermeyer K, Hawkes J, Einarsdóttir K, Kothawala D, Bergquist J, Tranvik L (2020) Selective Adsorption of Terrestrial Dissolved Organic Matter to Inorganic Surfaces Along a Boreal Inland Water Continuum. J Geophys Research: Biogeosciences 125:1–22.
- Hansen AM, Kraus TEC, Pellerin BA, Fleck JA, Downing BD, Bergamaschi BA (2016) Optical properties of dissolved organic matter (DOM): effects of biological and photolytic degradation. Limnol Oceanogr 61:1015–1032. https://doi.org/10.1002/lno.10270
- Harir M, Cawley KM, Hertkorn N, Schmitt-Kopplin P, Jaffé R (2022) Molecular and spectroscopic changes of peat-derived organic matter following photo-exposure: Effects on heteroatom composition of DOM. Sci Total Environ 838:155790. https://doi.org/10.1016/j. scitotenv.2022.155790
- Hawkes JA, Dittmar T, Patriarca C, Tranvik L, Bergquist J (2016) Evaluation of the Orbitrap Mass Spectrometer for the Molecular Fingerprinting Analysis of Natural Dissolved Organic Matter. Anal Chem 88:7698–7704. https://doi.org/10.1021/acs.analchem. 6b01624

- He D, Li P, He C, Wang Y, Shi Q (2022) Eutrophication and watershed characteristics shape changes in dissolved organic matter chemistry along two river-estuarine transects. Water Res 214:118196. https://doi.org/10.1016/j.watres.2022.118196
- Hernandez DR, Debord JD, Ridgeway ME, Kaplan DA, Park MA, Fernandez-Lima F (2014) Ion dynamics in a trapped ion mobility spectrometer. Analyst 139:1913–1921. https://doi.org/10.1039/C3AN02174B
- Hertkorn N, Harir M, Koch BP, Michalke B, Schmitt-Kopplin P (2013) High-field NMR spectroscopy and FTICR mass spectrometry: powerful discovery tools for the molecular level characterization of marine dissolved organic matter. Biogeosciences 10:1583–1624. https://doi.org/10.5194/bg-10-1583-2013
- Hertkorn N, Harir M, Cawley KM, Schmitt-Kopplin P, Jaffé R (2016) Molecular characterization of dissolved organic matter from subtropical wetlands: a comparative study through the analysis of optical properties, NMR and FTICR/MS. Biogeosciences 13:2257–2277. https://doi.org/10.5194/bg-13-2257-2016
- Herzsprung P, Hertkorn N, Von Tümpling W, Harir M, Friese K, Schmitt-Kopplin P (2014) Understanding molecular formula assignment of Fourier transform ion cyclotron resonance mass spectrometry data of natural organic matter from a chemical point of view. Anal Bioanal Chem 406:7977–7987. https://doi.org/10.1007/s00216-014-8249-y
- Hosen JD, Armstrong AW, Palmer MA (2018) Dissolved organic matter variations in coastal plain wetland watersheds: The integrated role of hydrological connectivity, land use, and seasonality. Hydrol Process 32:1664–1681. https://doi.org/10.1002/hyp.11519
- Jaffé R, Mead R, Hernandez ME, Peralba MC, Diguida OA (2001) Origin and transport of sedimentary organic matter in two subtropical estuaries: a comparative, biomarker-based study. Org Geochem 32:507–526. https://doi.org/10.1016/S0146-6380(00)00192-3
- Kellerman AM, Kothawala DN, Dittmar T, Tranvik LJ (2015) Persistence of dissolved organic matter in lakes related to its molecular characteristics. Nat Geosci 8:454–457. https://doi.org/10.1038/ngeo2440
- Koch BP, Dittmar T (2006) From mass to structure: an aromaticity index for high-resolution mass data of natural organic matter. Rapid Commun Mass Spectrom 20:926–932. https://doi.org/10. 1002/rcm.2386
- Koch BP, Witt M, Engbrodt R, Dittmar T, Kattner G (2005) Molecular formulae of marine and terrigenous dissolved organic matter detected by electrospray ionization Fourier transform ion cyclotron resonance mass spectrometry. Geochim Cosmochim Acta 69:3299–3308. https://doi.org/10.1016/j.gca.2005.02.027
- Kominoski JS, Gaiser EE, Castañeda-Moya E, Davis SE, Dessu SB, Julian Ii P, Lee DY, Marazzi L, Rivera-Monroy VH, Sola A, Stingl U, Stumpf S, Surratt D, Travieso R, Troxler TG (2020) Disturbance legacies increase and synchronize nutrient concentrations and bacterial productivity in coastal ecosystems. Ecology 101:1–13. https://doi.org/10.1002/ecy.2988
- Kujawinski EB, Del Vecchio R, Blough NV, Klein GC, Marshall AG (2004) Probing molecular-level transformations of dissolved organic matter: insights on photochemical degradation and protozoan modification of DOM from electrospray ionization Fourier transform ion cyclotron resonance mass spectrometry. Mar Chem 92:23–37. https://doi.org/10.1016/j.marchem.2004.06.038
- Law KP, He W, Tao J, Zhang C (2021) Characterization of the Exometabolome of Nitrosopumilus maritimus SCM1 by Liquid Chromatography–Ion Mobility Mass Spectrometry. Front Microbiol 12:1–20. https://doi.org/10.3389/fmicb.2021.658781
- Leyva D, Tose LV, Porter J, Wolff J, Jaffé R, Fernandez-Lima F (2019) Understanding the structural complexity of dissolved organic matter: isomeric diversity. Faraday Discuss 218:431–440. https://doi.org/10.1039/C8FD00221E



- Leyva D, Jaffe R, Fernandez-Lima F (2020) Structural Characterization of Dissolved Organic Matter at the Chemical Formula Level Using TIMS-FT-ICR MS/MS. Anal Chem 92:11960–11966. https://doi.org/10.1021/acs.analchem.0c02347
- Leyva D, Tariq MU, Jaffé R, Saeed F, Lima FF (2022) Unsupervised Structural Classification of Dissolved Organic Matter Based on Fragmentation Pathways. Environ Sci Technol 56:1458–1468. https://doi.org/10.1021/acs.est.1c04726
- Lu K, Gardner WS, Liu Z (2018) Molecular Structure Characterization of Riverine and Coastal Dissolved Organic Matter with Ion Mobility Quadrupole Time-of-Flight LCMS (IM Q-TOF LCMS). Environ Sci Technol 52:7182–7191. https://doi.org/10.1021/acs.est.8b00999
- Lu K, Li X, Chen H, Liu Z (2021) Constraints on isomers of dissolved organic matter in aquatic environments: Insights from ion mobility mass spectrometry. Geochim Cosmochim Acta 308:353–372. https://doi.org/10.1016/j.gca.2021.05.007
- Maie N, Yang C, Miyoshi T, Parish K, Jaffé R (2005) Chemical characteristics of dissolved organic matter in an oligotrophic subtropical wetland/estuarine. Limnol Oceanogr 50:23–35. https://doi.org/10.4319/lo.2005.50.1.0023
- Maie N, Pisani O, Jaffé R (2008) Mangrove tannins in aquatic ecosystems: Their fate and possible influence on dissolved organic carbon and nitrogen cycling. Limnol Oceanogr 53:160–171. https://doi.org/10.4319/lo.2008.53.1.0160
- Maie N, Sekiguchi S, Watanabe A, Tsutsuki K, Yamashita Y, Melling L, Cawley KM, Shima E, Jaffé R (2014) Dissolved organic matter dynamics in the oligo/meso-haline zone of wetland-influenced coastal rivers. J Sea Res 91:58–69. https://doi.org/10.1016/j. seares.2014.02.016
- Mcdaniel EW, Mason EA (1973) Mobility and diffusion of ions in gases. John Wiley and Sons, Inc, New York
- Medeiros PM, Seidel M, Ward ND, Carpenter EJ, Gomes HR, Niggemann J, Krusche AV, Richey JE, Yager PL, Dittmar T (2015) Fate of the Amazon River dissolved organic matter in the tropical Atlantic Ocean. Glob Biogeochem Cycles 29:677–690. https://doi.org/10.1002/2015GB005115
- Minor EC, Dalzell BJ, Stubbins A, Mopper K (2007) Evaluating the photoalteration of estuarine dissolved organic matter using direct temperature-resolved mass spectrometry and UV-visible spectroscopy. Aquat Sci 69:440–455. https://doi.org/10.1007/s00027-007-0897-y
- Morrison ES, Shields MR, Bianchi TS, Liu Y, Newman S, Tolic N, Chu RK (2020) Multiple biomarkers highlight the importance of water column processes in treatment wetland organic matter cycling. Water Res 168:115153. https://doi.org/10.1016/j.watres. 2019.115153
- Olanrewaju CA, Ramirez CE, Fernandez-Lima F (2021) Characterization of Deasphalted Crude Oils Using Gas Chromatography—Atmospheric Pressure Laser Ionization—Trapped Ion Mobility Spectrometry—Time-of-Flight Mass Spectrometry. Energy Fuels 35:13722–13730. https://doi.org/10.1021/acs.energyfuels.1c017
- Osterholz H, Niggemann J, Giebel H-A, Simon M, Dittmar T (2015) Inefficient microbial production of refractory dissolved organic matter in the ocean. Nat Commun 6:1–8. https://doi.org/10. 1038/ncomms8422
- Osterholz H, Kirchman DL, Niggemann J, Dittmar T (2016) Environmental drivers of dissolved organic matter molecular composition in the Delaware Estuary. Front Earth Sci 4:1–14. https://doi.org/10.3389/feart.2016.00095
- Osterholz H, Kirchman DL, Niggemann J, Dittmar T (2016b) Environmental Drivers of Dissolved Organic Matter Molecular Composition in the Delaware Estuary. Front Earth Sci 4:1–14.
- Patriarca C, Bergquist J, Sjöberg PJR, Tranvik L, Hawkes JA (2018) Online HPLC-ESI-HRMS Method for the Analysis and

- Comparison of Different Dissolved Organic Matter Samples. Environ Sci Technol 52:2091–2099.
- Petras D, Koester I, Da Silva R, Stephens BM, Haas AF, Nelson CE, Kelly LW, Aluwihare LI, Dorrestein PC (2017) High-Resolution Liquid Chromatography Tandem Mass Spectrometry Enables Large Scale Molecular Characterization of Dissolved Organic Matter. Front Mar Sci 4:1–14. https://doi.org/10.3389/fmars. 2017.00405
- Powers LC, Lapham LL, Malkin SY, Heyes A, Schmitt-Kopplin P, Gonsior M (2021) Molecular and optical characterization reveals the preservation and sulfurization of chemically diverse porewater dissolved organic matter in oligohaline and brackish Chesapeake Bay sediments. Org Geochem 161:1–15. https:// doi.org/10.1016/j.orggeochem.2021.104324
- Regier P, Jaffé R (2016) Short-Term Dissolved Organic Carbon Dynamics Reflect Tidal, Water Management, and Precipitation Patterns in a Subtropical Estuary. Front Mar Sci 3:1–14. https://doi.org/10.3389/fmars.2016.00250
- Regier P, Larsen L, Cawley K, Jaffé R (2020) Linking Hydrology and Dissolved Organic Matter Characteristics in a Subtropical Wetland: A Long-Term Study of the Florida Everglades. Glob Biogeochem Cycles 34:1–20. https://doi.org/10.1029/2020G B006648
- Ridgeway ME, Wolff JJ, Silveira JA, Lin C, Costello CE, Park MA (2016) Gated trapped ion mobility spectrometry coupled to fourier transform ion cyclotron resonance mass spectrometry. Int J Ion Mobil Spectrom 19:77–85. https://doi.org/10.1007/s12127-016-0197-0
- Robinson EW, Garcia DE, Leib RD, Williams ER (2006) Enhanced Mixture Analysis of Poly(ethylene glycol) Using High-Field Asymmetric Waveform Ion Mobility Spectrometry Combined with Fourier Transform Ion Cyclotron Resonance Mass Spectrometry. Anal Chem 78:2190–2198. https://doi.org/10.1021/ac051709x
- Roebuck JA, Seidel M, Dittmar T, Jaffé R (2018) Land Use Controls on the Spatial Variability of Dissolved Black Carbon in a Subtropical Watershed. Environ Sci Technol 52:8104–8114. https://doi.org/10.1021/acs.est.8b00190
- Ruotolo BT, Hyung S-J, Robinson PM, Giles K, Bateman RH, Robinson CV (2007) Ion Mobility–Mass Spectrometry Reveals Long-Lived, Unfolded Intermediates in the Dissociation of Protein Complexes. Angew Chem Int Ed 46:8001–8004. https://doi.org/10.1002/anie.200702161
- Schmidt F, Elvert M, Koch BP, Witt M, Hinrichs K-U (2009) Molecular characterization of dissolved organic matter in pore water of continental shelf sediments. Geochim Cosmochim Acta 73:3337–3358. https://doi.org/10.1016/j.gca.2009.03.008
- Schmidt F, Koch BP, Elvert M, Schmidt G, Witt M, Hinrichs K-U (2011) Diagenetic Transformation of Dissolved Organic Nitrogen Compounds under Contrasting Sedimentary Redox Conditions in the Black Sea. Environ Sci Technol 45:5223–5229. https://doi.org/10.1021/es2003414
- Schrader W, Xuan Y, Gaspar A (2014) Studying ultra-complex crude oil mixtures by using High Field Asymmetric Waveform Ion Mobility Spectrometry (FAIMS) coupled to an ESI-LTQ-Orbitrap Mass Spectrometer. Eur J Mass Spectrom 20:43–49.
- Seidel M, Beck M, Riedel T, Waska H, Suryaputra IGNA, Schnetger B, Niggemann J, Simon M, Dittmar T (2014) Biogeochemistry of dissolved organic matter in an anoxic intertidal creek bank. Geochim Cosmochim Acta 140:418–434.
- Seidel M, Yager PL, Ward ND, Carpenter EJ, Gomes HR, Krusche AV, Richey JE, Dittmar T, Medeiros PM (2015) Molecular-level changes of dissolved organic matter along the Amazon Riverto-ocean continuum. Mar Chem 177:218–231. https://doi.org/10.1016/j.marchem.2015.06.019



- Sleighter RL, Hatcher PG (2008) Molecular characterization of dissolved organic matter (DOM) along a river to ocean transect of the lower Chesapeake Bay by ultrahigh resolution electrospray ionization Fourier transform ion cyclotron resonance mass spectrometry. Mar Chem 110:140–152. https://doi.org/10.1016/j.marchem.2008.04.008
- Spranger T, Pinxteren DV, Reemtsma T, Lechtenfeld OJ, Herrmann H (2019) 2D Liquid Chromatographic Fractionation with Ultra-high Resolution MS Analysis Resolves a Vast Molecular Diversity of Tropospheric Particle Organics. Environ Sci Technol 53:11353–11363. https://doi.org/10.1021/acs.est.9b03839
- Stow SM, Causon TJ, Zheng X, Kurulugama RT, Mairinger T, May JC, Rennie EE, Baker ES, Smith RD, Mclean JA, Hann S, Fjeld-sted JC (2017) An Interlaboratory Evaluation of Drift Tube Ion Mobility–Mass Spectrometry Collision Cross Section Measurements. Anal Chem 89:9048–9055. https://doi.org/10.1021/acs.analchem.7b01729
- Stubbins A, Spencer RGM, Chen H, Hatcher PG, Mopper K, Hernes PJ, Mwamba VL, Mangangu AM, Wabakanghanzi JN, Six J (2010) Illuminated darkness: Molecular signatures of Congo River dissolved organic matter and its photochemical alteration as revealed by ultrahigh precision mass spectrometry. Limnol Oceanogr 55:1467–1477.
- Tose LV, Benigni P, Leyva D, Sundberg A, Ramírez CE, Ridgeway ME, Park MA, Romão W, Jaffé R, Fernandez-Lima F (2018) Coupling trapped ion mobility spectrometry to mass spectrometry: trapped ion mobility spectrometry-time-of-flight mass spectrometry versus trapped ion mobility spectrometry-Fourier transform ion cyclotron resonance mass spectrometry. Rapid Commun Mass Spectrom 32:1287–1295.
- Vannote RL, Minshall GW, Cummins KW, Sedell JR, Cushing CE (1980) The River Continuum Concept. Can J Fish Aquat Sci 37:130–137
- Venter P, Muller M, Vestner J, Stander MA, Tredoux AGJ, Pasch H, De Villiers A (2018) Comprehensive Three-Dimensional LC × LC × Ion Mobility Spectrometry Separation Combined with High-Resolution MS for the Analysis of Complex Samples. Anal Chem 90:11643–11650. https://doi.org/10.1021/acs.analchem.8b03234
- Wagner S, Jaffé R, Cawley K, Dittmar T, Stubbins A (2015) Associations Between the Molecular and Optical Properties of Dissolved Organic Matter in the Florida Everglades, a Model Coastal Wetland System. Front Chem 3:1–14. https://doi.org/10.3389/fchem. 2015.00066
- Wang C, Li Y, Li Y, Zhou H, Stubbins A, Dahlgren RA, Wang Z, Guo W (2021) Dissolvedorganic matter dynamics in the epipelagic northwest Pacific low-latitude westernboundary current system:

- insights from optical analyses. J Geophys Res 126:1–18. https://doi.org/10.1029/2021JC017458
- Ward CP, Cory RM (2016) Complete and Partial Photo-oxidation of Dissolved Organic Matter Draining Permafrost Soils. Environ Sci Technol 50:3545–3553. https://doi.org/10.1021/acs.est.5b05354
- Ward ND, Keil RG, Medeiros PM, Brito DC, Cunha AC, Dittmar T, Yager PL, Krusche AV, Richey JE (2013) Degradation of terrestrially derived macromolecules in the Amazon River. Nat Geosci 6:530–533. https://doi.org/10.1038/ngeo1817
- Wilske C, Herzsprung P, Lechtenfeld OJ, Kamjunke N, Von Tümpling W (2020) Photochemically Induced Changes of Dissolved Organic Matter in a Humic-Rich and Forested Stream. Water 12:1–21.
- Ya C, Anderson W, Jaffé R (2015) Assessing dissolved organic matter dynamics and source strengths in a subtropical estuary: Application of stable carbon isotopes and optical properties. Cont Shelf Res 92:98–107.
- Yamashita Y, Scinto LJ, Maie N, Jaffé R (2010) Dissolved Organic Matter Characteristics Across a Subtropical Wetland's Landscape: Application of Optical Properties in the Assessment of Environmental Dynamics. Ecosystems 13:1006–1019. https://doi.org/10. 1007/s10021-010-9370-1
- Yamashita Y, Boyer JN, Jaffé R (2013) Evaluating the distribution of terrestrial dissolved organic matter in a complex coastal ecosystem using fluorescence spectroscopy. Cont Shelf Res 66:136–144. https://doi.org/10.1016/j.csr.2013.06.010
- Zhang Y, Zhou Y, Shi K, Qin B, Yao X, Zhang Y (2018) Optical properties and composition changes in chromophoric dissolved organic matter along trophic gradients: Implications for monitoring and assessing lake eutrophication. Water Res 131:255–263. https://doi.org/10.1016/j.watres.2017.12.051
- Zhang X, Cao F, Huang Y, Tang J (2022) Variability of dissolved organic matter in two coastal wetlands along the Changjiang River Estuary: Responses to tidal cycles, seasons, and degradation processes. Sci Total Environ 807:1–14. https://doi.org/10.1016/j.scito tenv.2021.150993

Publisher's Note Springer Nature remains neutral with regard to jurisdictional claims in published maps and institutional affiliations.

Springer Nature or its licensor holds exclusive rights to this article under a publishing agreement with the author(s) or other rightsholder(s); author self-archiving of the accepted manuscript version of this article is solely governed by the terms of such publishing agreement and applicable law.

